Published online 26 July 2008

Nucleic Acids Research, 2008, Vol. 36, No. 15 ***5021–5032***
doi:10.1093/nar/gkn426

Multimolecular complex of *Par-4* and E2F1 binding to *Smac* promoter contributes to glutamate-induced apoptosis in human-bone mesenchymal stem cells

Chao Lu*, Jie-Qing Chen, Guo-Ping Zhou, Sheng-Hua Wu, Ya-Fei Guan and Chuan-Shun Yuan

Department of Pediatrics, the First Affiliated Hospital of Nanjing Medical University, Nanjing, Jiangsu, 210029, People's Republic of China

Received March 18, 2008; Revised June 1, 2008; Accepted June 17, 2008

ABSTRACT

Neural cells undergo glutamate-induced apoptosis in ischaemic brain tissue, in which prostate apoptosis response-4 gene (*Par-4*) is involved. Human-bone mesenchymal stem cells can be utilized as an effective therapy for ischemic brain injury. In this study, we found that glutamate could induce apoptosis in human-bone mesenchymal stem cells, accompanied by increased expression of *Par-4* gene and *Smac* release from mitochondria. Repressing *Par-4* expression attenuated the glutamate-induced apoptosis. Both *Par-4* protein and E2F1 protein could bind to E2F1-binding BS3 site on *Smac* promoter and participated in the formation of a proteins-DNA complex. Moreover, in the complex, E2F1, not *Par-4*, was found to be directly bound to the *Smac* promoter, suggesting that *Par-4* exerted indirectly its transcriptional control on the *Smac* gene though interacting with E2F1. Expression of full-length *Par-4* in human-bone mesenchymal cells resulted in increased activity of the *Smac* promoter. In addition, the indirect transcripional regulation of *Par-4* on *Smac* depended on its COOH terminus-mediated interaction between *Par-4* and E2F1. We conclude that the formation of proteins–DNA complex, containing *Par-4* protein, E2F1 protein and the *Smac* promoter, contributes to the pro-apoptotic effect on glutamate-treated human-bone mesenchymal stem cells.

INTRODUCTION

As a major contributor to death and disability, ischaemic brain injury does not only affect adults (1,2), it is also an important cause of mortality and severe neurodevelopmental morbidity in children, such as cerebral palsy, mental retardation, epilepsy and learning disability (3). Human-bone mesenchymal stem cells (hBMSCs) are self-renewing multipotent cells, which can be utilized as an effective therapy for ischemic brain injury. However, although considerable studies have been devoted to investigating the therapeutic efficacy of hBMSCs transplantation in ischemic brain, rather less attention has been paid to the biochemical regulation of the stem cell itself in a pro-apoptotic microenvironment of ischaemic brain tissue. Thus, it is of paramount importance to investigate the events and factors that predispose hBMSCs to undergo apoptosis in ischaemia tissue.

Glutamate, an excitatory amino acid, binds to postsynaptically located glutamate receptors that regulate calcium channels in ischaemic brain tissue. The resulting calcium influx activates proteases, lipases and endonucleases, which in turn destroy the cellular skeleton, finally leading to cells necrosis or switch on apoptosis (4). The implanted stem cells will suffer from the impairment of excitotoxic glutamate as well in such a microenvironment. Hence, for alleviating suffering and improving survival of implanted cells in ischaemic brain tissue, it is important to determine how hBMSCs respond to glutamate.

The *prostate apoptosis response factor-4* (*Par-4*) gene was originally identified by differential screening for up-regulated genes in apoptotic prostate cell (5). Subsequently, *Par-4* was found to possess potent apoptotic activity in various cellular systems. In the past few years, several studies have investigated the role of *Par-4* in cell apoptosis and found that *Par-4* had been attributed a crucial function to its COOH terminus domain (6,8). One of the most noticeable structural features of *Par-4* COOH terminus was the leucine zipper repeats, a putative death domain, which was found in several other proteins involved in apoptosis, suggesting the importance of this region in *Par-4* function (7,9). However, despite the advances made in understanding the role of *Par-4* in apoptosis, little was known about whether *Par-4* is involved in the response of glutamate-treated hBMSCs.

*To whom correspondence should be addressed. Tel: +86 25 13505169395; Fax: +86 25 86291273; Email: luchao8009@163.com

Smac (the *second mitochondria-derived activator of caspase*), also known as *DIABLO* (*direct IAP-binding protein with low pI*), is a pro-apoptotic protein and is normally compartmentalized and stored in mitochondria upon receiving apoptotic stimuli; *Smac* is released into cytosol, where it binds to IAPs, and active caspases either by eradicating the binding capability of IAPs to caspases or enhancing the proteosome-mediated degradation of IAPs (10,11). In addition, E2F1, a member of E2F transcription factor family, can bind to the *Smac* promoter and transcriptionlly upregulate *Smac* expression, which results into the mitochondria-mediated apoptosis (12). However, it remains unclear whether *Smac* plays a role in glutamate-induced hBMSCs apoptosis.

In this study, we demonstrate for the first time that excitotoxic glutamate can induce hBMSCs apoptosis, accompanied by increased expression of *Par-4* and *Smac* release from mitochondria. Our results indicate that the glutamate-induced pro-apoptotic effect on hBMSCs is partially due to the formation of multimolecular complex of *Par-4*, E2F1 and *Smac* promoter. Our results show that *Par-4* can transcriptionally modulate *Smac* expression through the indirect interaction between *Par-4* and *Smac* promoter. The association of *Par-4* with E2F1 which depended on the COOH terminus of *Par-4*, enhances the capability of E2F1 binding to *Smac* promoter. In conclusion, our findings provided the detailed molecular mechanisms responsible for glutamate-induced apoptosis in hBMSCs.

MATERIALS AND METHODS

Reagents and antibodies

Par-4 rabbit polyclonal antibody, E2F1 rabbit polyclonal antibody and FITC conjugated anti-rabbit IgG secondary antibodies were purchased from Santa Cruz Biotechnology (Santa Cruz, CA, USA). The majority of reagents used for this study, including glutamate and DAPI, were obtained from Sigma–Aldrich (St Louis, MO, USA). Anti-CD105 (endoglin), -CD73, -CD106 (VCAM-1), -CD44,-CD90, -CD29, -CD45, -CD14, -CD34, -CD80, -CD86 antibodies, were purchased from BD Biosciences (La Jolla, CA, USA). pGEMT-easy vector, Gel Shift Assay kit, pGL3 Luciferase Reporter Vector were obtained from Promega (Madison, WI, USA). Advantage 2 DNA polymerase and pcDNA3.1/myc-his vector were obtained from BD Biosciences (La Jolla, CA, USA). Restriction endonucleases were purchased from New England BioLab (Beverly, MA, USA). Endo-free Plasmid Maxi kit was obtained from Qiagen (Hilden, Germany). Lipofectamine 2000 reagent was obtained from Invitrogen (Carlsbad, CA, USA). Nuclear Protein Extraction kit was purchased from Active Motif (Carlsbad, CA, USA).

Cell culture and hBMSCs phenotype analysis

Culture and characterization of hBMSCs were performed as described previously (13). Briefly, bone marrow cells were obtained from 5 ml aspirates from the iliac crest of normal donors after informed consents were given. Cells were plated at a density of 5×10^6 per 25 cm^2 flask in 5 ml Dulbecco's modified Eagle's medium (DMEM) supplemented with 100 μg/ml penicillin, 100 μg/ml streptomycin and 10% fetal calf serum, incubated at 37°C in a humidified atmosphere containing 5% CO_2. After 72 h, non-adherent cells were discarded and adherent cells were washed gently with DMEM medium and cultured for ~21 days. The culture medium was replaced with fresh complete medium twice a week. Upon reaching near confluence, cells were detached with a solution of 0.25% trypsin and 100 μMol/l EDTA for 2–3 min at 37°C and plated at 1000 cells/cm^2 with medium replacement twice a week. Cells used in our experiments were the fifth or sixth passage of cultivation. hBMSCs were immunophenotyped by fluorescence-activated cell sorting (FACS). Cells were detached with trypsin-EDTA, washed in PBS, and immediately stained with the following labelled antibodies: CD105-FITC, CD73-FITC, CD44-FITC, CD90-FITC, CD147-FITC, HLA Class I-FITC, CD29-FITC, CD34-PE, CD45-PE, CD14-PE, CD11b-PE and HLA-DR-PE and then analysed using a flow cytometry.

Fluorescence-activated cell sorter analysis

hBMSCs were harvested in the presence or absence of 1—100 μM glutamate for 6, 12 or 24 h. Cells were collected by trypsinization and washed in PBS. After incubation with 5 μl of Annexin V-FITC and 10 μl of propidium iodide (PI, 50 μg/ml) at room temperature for 15 min in the dark, cells were analysed by flow cytometry. The percentages of apoptosis in the cells were calculated by data from FACS analysis and the result is presented in the bar graph relative to the apoptotic cell rate in hBMSCs without treatment of glutamate.

DNA fragmentation assay

DNA fragmentation was assessed using a soluble DNA preparation as previously described (14). hBMSCs were harvested in the presence or absence of 100 μM glutamate for 24 h. Then cells were lysed in 10 mM Tris–HCl (pH 7.5) containing 10 mM EDTA and 0.2% Triton X-100. The lysate was centrifuged at 12 000*g* for 10 min. The supernatant was treated with proteinase K (0.3 mg/ml) and RNase A (0.3 mg/ml) and then extracted in the presence of 300 mM NaAc. The DNA was precipitated with isopropanol and dissolved in 10 mM Tris–HCl (pH 8.0) containing 100 μM EDTA. The DNA was electrophoresed in 1.5% agarose gel in Tris borate-EDTA buffer. The DNA bands were then imaged by ethidium bromide staining and photographed.

Subcellular fractionation

Cells were washed once in PBS and harvested in isotonic buffer (250 mM sucrose, 1 mM EDTA and 10 mM HEPES, pH 7.4) supplemented with 0.25 mM phenylmethylsulfonyl fluoride, 10 μg/ml leupeptin and 10 μg/ml aprotinin. After a brief sonication, samples were transferred to 1.5-ml tubes and centrifuged at 900*g* for 10 min at 4°C to eliminate nuclei and unbroken cells. Supernatant was then centrifuged at 9500*g* for 15 min at 4°C to obtain the heavy membrane pellet enriched for mitochondria,

and the resulting supernatant was stored as the cytosolic fraction.

Western blotting analysis

Cells were collected by trypsinization and washed in PBS. Then cell pellets were lysed in 1% Nonidet P-40 lysis buffer (150 mM NaCl, 1% Nonidet P-40, 0.5% sodium deoxycholate, 0.1% SDS, 50 mM Tris, pH 8.0), to which 2 mM phenylmethylsulfonyl fluoride, 3.3 μg/ml leupeptin and 5 μg/ml pepstatin were added fresh before use. Fifty micrograms of proteins was loaded on precast SDS/Tris/glycine gels, and after electrophoresis, proteins were transferred to nitrocellulose membranes, which were blocked in 5% non-fat dry milk and blotted with the appropriate primary antibody. Membranes were then incubated with the appropriate secondary antibody linked to horseradish peroxidase and developed using the ECL kit according to the manufacturers' protocols. *Smac* levels were represented as ratios between the levels in mitochondria versus cytosol.

Small interfering RNA-based (siRNA) experiments

A small interfering RNA-based (siRNA) strategy was employed to silence endogenous human *Par-4* in hBMSCs. *Par-4* and scrambled siRNAs were generated using the procedure of siSTRIKE™ U6 Hairpin Cloning Systems (Promega, Madison, WI). The four siRNAs had the following sense strand sequences:

Par-4-siRNA-1:
5′-ACCGTCACAGCCGTTTGAATATATTTCAAGAGAATATATTCAAACGGCTGTGACTTTTTC-3′.

Par-4-siRNA-2:
5′-ACCGGAAACGAGAAGATGCAATTATTCAAGAGATAATTGCATCTTCTCGTTTCCTTTTTC-3′.

Par-4-siRNA-3:
5′-ACCGTGAGACTGATGCAAGATAAATTCAAGAGATTTATCTTGCATCAGTCTCACTTTTTC-3′.

Par-4-siRNA-4:
5′-ACCGAACAGTTTCAGGCAGATATATTCAAGAGATATATCTGCCTGAAACTGTTCTTTTTC-3′.

The target sequences for the *Par-4* gene are underlined. Sense and antisense strands were annealed and ligated into linearized psiSTRIKE Vector following the manufacturer's directions. Sequence analysis of transformed randomly picked clones was used to confirm sequence integrity of *Par-4* siRNA plasmids. Cells were transfected with siRNA or the indicated constructs using Lipofectamine 2000 in Opti-MEM I for 24 h, and then the medium was changed back to growth medium for additional incubation. Green fluorescent protein phMGFP vector was cotransfected to determine transfection efficiency with flow cytometry assay. Forty-eight hours after transfection, total RNA was prepared and used to perform real time quantitative PCR analysis. The level of target RNA suppression in transfected cells were determined by normalizing for transfection efficiency. Small interfering RNA-based experiment for *Smac* and E2F1 were similarly performed.

RT–PCR analysis

Cells were harvested, and total RNA extraction was performed. RNA purity (A260/A280 >1.6) was checked by a spectrophotometer (GeneQuant, Type II; Pharmacia, Uppsala, Sweden), and RNA integrity was confirmed by visualization of 28 and 18 s bands (2:1) on 1% agarose gel. Subsequently, 1 μg of RNA was reverse transcribed using the Moloney-murine leukaemia virus reverse transcription system. The beta-actin was used as internal controls. PCR reactions were performed in a 50 μl mixture containing 10 × PCR buffer, MgCl2, dNTP, and Taq DNA polymerase. Amplification protocols for *Smac* and beta-actin consisted of 30 repetitive cycles of pre-denaturing at 95°C for 4 min, denaturing at 94°C for 30 s and annealing at 60°C for 60 s. Amplified cDNA was separated by 2% agarose gel electrophoresis and visualized with ethidium bromide. Semiquantitative analysis was performed using UVP-gel densitometry (San Gabriel, CA, USA). Arbitrary unit = $(A_{Smac}/A_{\text{beta-actin}})\times 100\%$.

Real time quantitative PCR

Total RNA extraction was performed using TriZol reagent followed by chloroform-isopropanol extraction and ethanol precipitation. Subsequently, duplicate samples of 1 μl of each cDNA were used as a template. Real time quantitative PCR was performed using the ABI PRISM 7700 sequence detection system (PE Applied Biosystems, Wellesley, MA, USA). We used primers and a probe generated by the program Primer Premier. *Par-4* primers were F (forward) 5-GCCGCAGAGTGCTTAGATGAG-3 and *Par-4* R (reverse) 5-GCAGATAGGAACTGCCTGGATC-3 (fragment length, 136 bp). TaqMan probe (FAM-labelled 5-ACGAAGATGATGAAGCAGGGCAGAAAGAG-3) was added to the PCR mixture to a final concentration of 200 nM. GAPDH primers were F (forward) 5-GAAGGTGAAGGTCGGAGTC-3 and GAPDH R (reverse) 5-GAAGATGGTGATGGGATTC-3 and GAPDH TaqMan probe fluorescence labeled 5F 5-CAAGCTTCCCGTTCTCAGCC-3 were used as internal controls. Amplification conditions were as follows: 50°C for 2 min, 95°C for 10 min and then 40 cycles at 95°C for 15 s and 60°C for 60 s. GAPDH was co-amplified with *Par-4*. Average threshold cycle (Ct) values from the triplicate PCR reactions for *Par-4* were normalized against the average Ct values for GAPDH from the same cDNA sample. The fold change of *Par-4* transcript levels between *Par-4*-siRNA-1,2,3,4 and the control equals $2^{-\Delta\Delta Ct}$, where $\Delta Ct = \text{Ct}_{Par\text{-}4} - \text{Ct}_{\text{GAPDH}}$, and $\Delta\Delta Ct = \Delta\Delta Ct_{\text{control}} - \Delta Ct_{Par\text{-}4\text{-siRNA-1,2,3,4}}$. Real time quantitative PCR for *Smac* was similarly performed.

Construction of expression plasmids and transient transfection

To construct and clone the eukaryotic expression vector of human *Par-4*, full-length cDNA of *Par-4* was amplified by Rt–PCR from human neuroblastoma cell line SK-N-SH (Shanghai Institute of Cell Biology, Chinese Academy of Science, Shanghai, Peoples' Republic of China).

After Rt–PCR amplification, *Par-4* cDNA was inserted to plasmid pGEM-T and transformed into *Escherichia coli* JM109. Positive clones were amplified, screened and identified by sequencing. Then *Par-4* cDNA was subcloned into pcDNA3.1 vector between the restriction enzyme sites HindIII and XhoI to generate the pcDNA3.1-*Par-4* construct. For construction of pcDNA3.1-myc-*Par-4*, which coded a myc-tagged *Par-4*, Rt–PCR amplification was performed with another pair of primers, from which the stop codon of *Par-4* was removed. pcDNA3.1-myc-Δ*Par-4* was similarly constructed, which encoded a myc fusion protein containing a *Par-4* deletion mutant, the latter lacking 70 amino acids at the COOH terminus of *Par-4*. Transfections were performed using the Lipofectamine 2000 procedure following the manufacturer's protocol. Green fluorescent protein phMGFP vector was cotransfected to determine transfection efficiency with flow cytometry assay.

Northern blotting analysis

Samples of total RNA (10 μg) were separated by electrophoresis through denaturing 1.2% agarose gels containing 1% formaldehyde and transferred onto nylon or nitrocellulose membranes using standard molecular biological techniques. Probes were derived from PCR products amplified with gene-specific primers for human *Smac* cDNA and labeled with [α-^{32}P]dCTP using the Prime-It random priming kit (Stratagene, La Jolla, CA). Filters were reprobed with the cDNA for GAPDH to correct for the amount of RNA loaded onto the filters. Pre-hybridization and hybridization were performed at 62°C for 1 h and overnight, respectively. The blot was subjected to low and high stringency washes using the buffers provided in the NorthernMaxTM kit for Northern blots (Ambion Inc., Inc., Austin, TX). After hybridization, the membranes were washed and exposed at −70°C to X-ray film using an intensifying screen.

Immunoprecipitations

Cells were lysed in icecold immunoprecipitation buffer (20 mM Tris–Cl (pH 7.5), 150 mM NaCl, 10% glycerol, 0.2% Nonidet P-40, and a protease inhibitor mixture (Roche Applied Science, Indianapolis, IN, USA). Lysis with immunoprecipitation buffer was complemented with sonication (5 pulses) on ice. The lysate was cleared of cell debris by centrifugation at 16 000*g* at 4°C for 30 min. The supernatant was saved for immunoprecipitation using anti-*Par-4* or anti-E2F1 conjugated to Sepharose beads overnight at 4°C with gentle agitation. The beads were washed 3 times in lysis buffer, resuspended in 2 × Laemmli buffer and boiled for 5 min to release bound proteins. Proteins were analysed by SDS–PAGE and immunoblotting after transfer to polyvinylidene difluoride membranes.

Isolation of nuclear proteins binding to biotinylated probes

Nuclear proteins binding to biotinylated probes were isolated as described previously (28). Briefly, oligonucleotides representing E2F1-binding site on *Smac* promoter sequence were synthesized, and 5 μg of the sense strand was 3′-labelled using the terminal deoxynucleotidyltransferase and biotin-14-dATP. The biotin-labelled sense strand was annealed to its complementary antisense strand and purified over a Sephadex column. The concentration of purified oligonucleotide was measured by absorbance at 260 nm, and equal amounts of annealed oligonucleotide were incubated with streptavidin-coated magnetic beads (Promega) for 30 min at room temperature. Coupling of the oligonucleotides to the beads was measured by absorbance. For the binding reaction, 50 μg of nuclear extract alone or preincubated with anti-*Par-4* antibody (R334) was used. The beads were captured by a magnet, washed three times with a high salt buffer, and resuspended in Laemmli buffer. The samples were heated at 95°C for 5 min to elute all the proteins, loaded onto a 12% SDS–PAGE, electrophoresed, and transferred to a nitrocellulose membrane. *Par-4* and E2F1 were detected using the *Par-4* antibody (R334) or E2F1 antibody by immunoblotting.

Nuclear extract preparation and electrophoretic mobility shift assays (EMSA)

The double-stranded oligonucleotides used for EMSA of E2F1-binding sites in *Smac* promoter are shown as follows: E2F1-binding BS3 site (underlined), 5′-GCCCC **GCGCGGAA**GTT-3′; mutated E2F1-binding BS3 site (underlined and in boldface), 5′-GCCCC**GCTTAGAA** GTT-3′; E2F1-binding BS2 site (underlined), 5′-GCG CAGCGCGATGCCGG-3′. The oligonucleotides were 5′-end-labeled with [γ-^{32}P]dATP. Nuclear proteins were extracted using a Nuclear Protein Extraction Kit. Electrophoretic mobility shift assay was performed by using a Gel Shift Assay Kit following the manufacturer's instructions. The nuclear extracts containing 30 μg of total proteins were preincubated with gel shift binding buffer for 10 min, followed by the addition of 1 μl of a [γ-^{32}P]-labelled, double-stranded oligonucleotide probe of E2F1 and incubation for 1h. Formed nuclear protein–DNA complexes were dissolved in 4% nondenaturing polyacrylamide gels, and electrophoresis was performed under 90 V for 2 h. Gels were dried and exposed to Kodak Biomax films at −70°C for 48 h. To assess the specificity of the reaction, competition assays were performed with 100-fold excess of unlabeled consensus oligonucleotide pairs of E2F1. The unlabelled probes were added to binding reaction mixture 10 min before the addition of the labelled probes. For the blocking reaction, 500 ng each of anti-*Par-4* antibody (R334) and anti-E2F1 antibody were used.

Chromatin immunoprecipitation

hBMSCs cultured in the presence or absence of 100 μM of glutamate for 24 h were subjected to chromatin immunoprecipitation. Chromatin immunoprecipitation was done as described earlier (28). Cells were plated in a 100-mm dish. About 70% confluent dishes were treated with formaldehyde (1%) for 10 min at 37°C to cross-link proteins to DNA. The cells were washed twice with PBS, pH 7.4, containing protease/inhibitor mixture (Roche Applied Science) and then lysed with lysis buffer containing 1% SDS. Sonication of cross-linked chromatin was performed

at 30% of maximum power with two rounds of 10 s pulses so that chromatin fragments thus obtained ranged from 500 to 2000 bp in size. Soluble chromatin was subjected to overnight immunoprecipitation with either anti-E2F1 antibody or anti-*Par-4* antibody. A portion of the chromatin solution was kept to check the amount of input DNA in different samples before immunoprecipitation. Following immunoprecipitation and elution, the eluent was heated to 65°C for 6 h to reverse the cross-link. Phenol/chloroform extraction was performed, and the supernatant was ethanol-precipitated. DNA thus obtained was resuspended in 10 mM Tris, 1 mM EDTA, pH 8.0 and subjected to PCR. Forward and reverse primers selected for *Smac* promoter are as follows: sense primer, 5′-TTC CCTTCAAGCCCTGGCCCGAAC-3′; antisense primer, 5′-ACGCCCCCACCCAAGGAAGCAGTC-3′; PCR products were resolved on a 1.5% agarose gel and stained with ethidium bromide.

Luciferase assays

pGL3-*Smac*-P-Luc reporter was constructed as described previously (28). Briefly, the *Smac* promoter fragment (−600 to −100 bp), which contained E2F1-binding BS3 site, was cloned into the Xho I/Hind III site of pGL3-Basic plasmid with the primer pairs indicated below. Sense, 5′-CCGCTCGAGCCGTCCGCCCCTCTGGGAC GGCGC-3′; Antisense, 5′-CGCAAGCTTAGCAGTCGG GATTGGGCAGGC-3′. hBMSCs were transiently cotransfected with appropriate pGL3-*Smac*-P-Luc reporter plasmids (200 ng) and either pcDNA3.1-myc-*Par-4* or pcDNA3.1-myc-Δ*Par-4* (200 ng) using Lipofectamine 2000. In each transfection, cells were also cotransfected with *Renilla* luciferase reporter plasmid pRL-CMV, which served as an internal control for transfection efficiency. Cell extracts were assayed for firefly and *Renilla* luciferase activity. Fold-activation values were measured relative to the levels of luciferase activity in cells transfected with empty vectors and normalized by *Renilla* luciferase activities.

RESULTS

Par-4 played an important role in glutamate-induced hBMSCs apoptosis

We investigated whether glutamate could induce apoptosis in hBMSCs. The cells were exposed continuously to 1–100 μM glutamate with different time lengths. Upon FACS analysis, we found that glutamate induced a dose-dependent apoptosis in hBMSCs, which started at 1 μM and peaked at 100 μM (Figure 1A), and glutamate at 100 μM induced a time-dependent cells apoptosis starting at 6 h and culminating at 24 h (Figure 1A and Supplementary Figure S1), which was confirmed by the following DNA laddering assay. As shown in Figure 1B, after exposure to 100 μM glutamate for 24 h, nucleosomal DNA fragmentation, an end stage apoptotic event, was observed in hBMSCs. By contrast, no DNA laddering was found in the cells without treatment of glutamate. These data showed that glutamate could induce apoptosis in hBMSCs.

To examine whether *Par-4* was involved in the regulation of glutamate-induced apoptosis in hBMSCs, Western blotting was performed to detect *Par-4* expression in the cells treated with or without glutamate. Because the pro-apoptotic function of *Par-4* was attributed to its nuclear translocation (13), Western blotting was performed with nuclear extracts. As shown in Figure 1C, glutamate induced a dose-dependent increase of *Par-4* expression in hBMSCs as compared with control.

To further confirm the role of *Par-4* in glutamate-induced apoptosis, we studied the effect of reducing *Par-4* expression on apoptosis of hBMSCs after treatment with glutamate. hBMSCs was transfected with either *Par-4* specific siRNA, scrambled siRNA, or no siRNA (Mock). The mRNA expression levels of *Par-4* in transected cells were assessed by real time quantitative PCR analysis. As shown in Figure 1D and Supplementary Figure S2, *Par-4*-siRNA-1, one of the tested siRNA, caused an effective reduction of *Par-4* mRNA. In all, 93% of *Par-4* mRNA was suppressed by *Par-4*-siRNA-1. Then, the transfected hBMSCs were treated with or without equal concentration of glutamate (100 μM) for 24 h. FACS analysis showed that the suppression of *Par-4* expression significantly attenuated the glutamate–induced apoptosis (Figure 1E and Supplementary Figure S3). By contrast, transient overexpression of *Par-4* increased the apoptosis cells in glutamate-treated hBMSCs (Figure 1F). Together, these data indicated that *Par-4* played an important role in glutamate-induced hBMSCs apoptosis.

Ectopic expression of *Par-4* enhanced the expression of *Smac*, which could be abrogated by blocking endogenous E2F1

To determine whether *Smac* is involved in glutamate-induced hBMSCs apoptosis, Western blotting was performed to detect the release of *Smac* from mitochondria. Figure 2A showed that *Smac* protein releasing from mitochondria exhibited an apparent increase upon the treatment with glutamate in a dose-dependent manner.

We next examined the relationship between *Par-4* and *Smac*. hBMSCs were transfected with plasmid pcDNA3.1-*Par-4*, which contained complete *Par-4* CDS. The same amount of empty pcDNA3 vector was also introduced into cells as a control. *Smac* protein expression was found to be upmodulated in the *Par-4* overexpressing hBMSCs (Figure 2B and Supplementary Figure S4). Northern blotting showed that *Smac* transcript in hBMSCs was enhanced as well (Figure 2C), suggesting a previously undefined transcriptional mechanism that *Par-4* could mediate upmodulation of *Smac* protein.

To characterize the involvement of E2F1 in the regulation of *Smac* in hBMSCs, we blocked the expression of endogenous E2F1 protein using siRNA. hBMSCs were cotransfected with pcDNA3-*Par-4* and plasmid pSiRNA-E2F1-1, the latter specifically targeting E2F1 for gene silencing. Western blotting analysis demonstrated *Smac* expression was restrained following the inhibition of

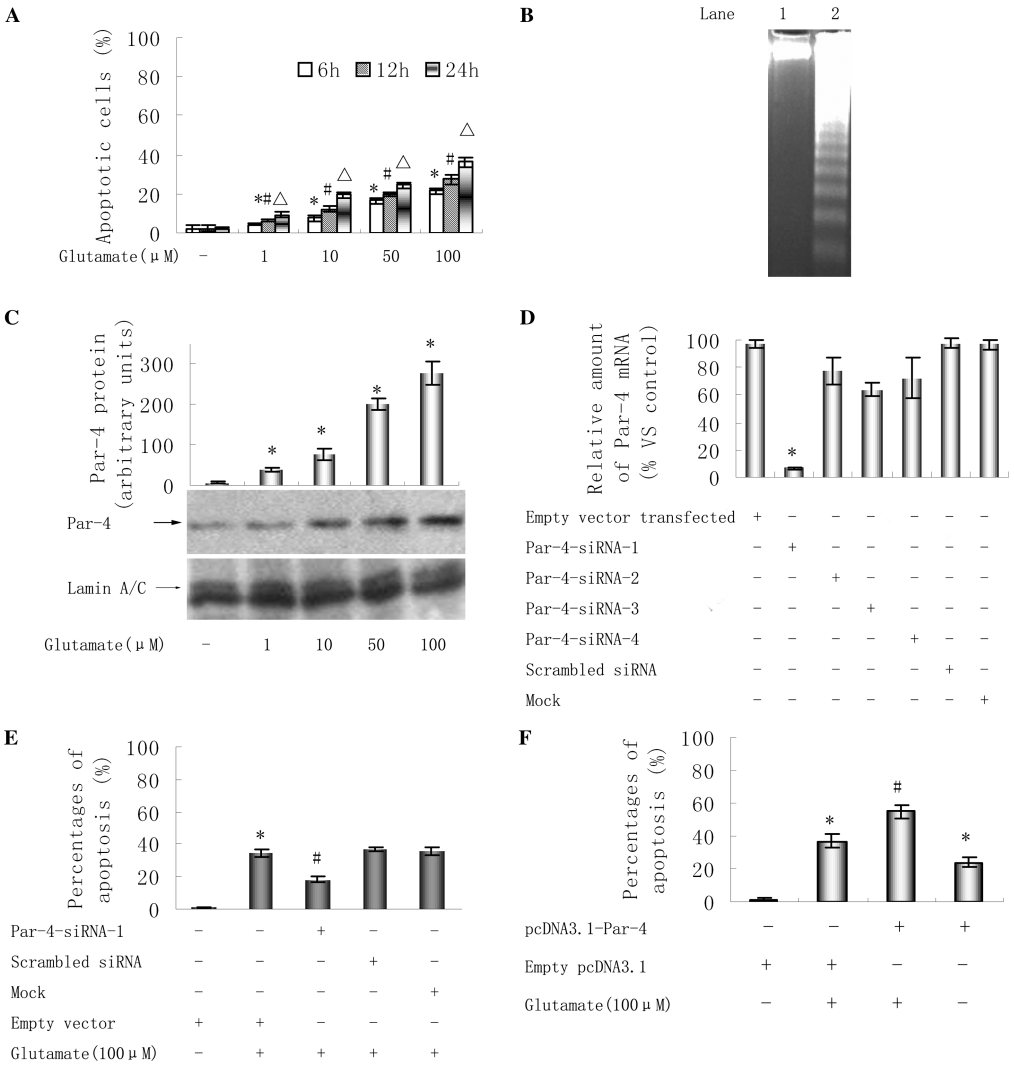

Figure 1. Par-4 plays an important role in glutamate-induced apoptosis of hBMSCs. (A) Glutamate induced apoptosis in hBMSCs. hBMSCs were harvested after treatment with or without 1–100 μM glutamate for 6, 12 or 24 h. Cells were incubated with Annexin V-FITC and propidium iodide and analysed by flow cytometry. The percentages of apoptotic cells are presented in the bar graph. Results are means of triplicates and representative for results of three independent experiments. *, #, Δ, $P < 0.05$. (**B**) DNA Fragmentation assay in apoptotic hBMSCs. hBMSCs were harvested after treatment with (lane 1) or without (lane 2) 100 μM glutamate for 24 h. DNA were precipitated and electrophoresed in 1.5% agarose gel. (**C**) Glutamate induced an increase of *Par-4* expression in hBMSCs in a dose-dependent manner. Western blotting analysis was used to determine *Par-4* expression in nuclear extracts in hBMSCs exposed to various doses of glutamate. Intensity of *Par-4* band from Western blotting were quantified and normalized with Lamin A/C. $^{*}P < 0.05$, compared to the hBMSCs without treatment of glutamate. (**D**) Real time Quantitative PCR assays for inhibitory effect of siRNA targeting *Par-4* gene. hBMSCs were transfected with either *Par-4* siRNA-1,2,3,4, scrambled siRNA or mock. Empty vector was transfected as a control. After 48 h of transfection, relative amounts of *Par-4* mRNA were measured by real-time quantitative RT–PCR and normalized against GAPDH. Bars depict the percentage of *Par-4* mRNA versus control. $^{*}P < 0.05$, versus control. (**E**) Reduced *Par-4* expression by siRNA inhibited glutamate-induced apoptosis of hBMSCs. hBMSCs were transfected with either *Par-4*-siRNA-1, scrambled siRNA or mock. After 48 h of transfection, hBMSCs were harvested in the presence or absence of 100 μM glutamate for 24 h. The percentages of apoptosis in the cells were analysed by flow cytometry. The result is presented in the bar graph. Values are mean ± SE of five independent experiments. $^{*}P < 0.05$, compared to the cells with transfection of empty vector but without exposure of glutamate. $^{\#}P < 0.05$, compared to the cells with transfection of empty vector and with exposure of glutamate. (**F**) Overexpression of *Par-4* predisposed hBMSCs to undergo apoptosis induced by glutamate. hBMSCs were transfected with either pcDNA3.1-*Par-4* or empty vector pcDNA3.1. After 48 h of transfection, hBMSCs were exposed to 100 μM glutamate for 24 h. The percentages of apoptosis in the cells were analysed by flow cytometry. $^{*}P < 0.05$, compared to the cells with transfection of empty pcDNA3.1 but without exposure of glutamate. $^{\#}P < 0.05$, compared to the cells with transfection of empty pcDNA3.1 and with exposure of glutamate.

E2F1 expression (Figure 2D and Supplementary Figure S5). Real time quantitative RT–PCR showed that pSiRNA-E2F1-1 could represse pcDNA3-*Par-4*-induced increase of *Smac* mRNA transcription (Figure 2E). These data indicated that E2F1 participated in *Par-4*-induced *Smac* transcription and expression.

Par-4 and E2F1 formed a protein complex in glutamate-treated hBMSCs

Based on the strong correlation among *Par-4*, E2F1 and *Smac* from our above study, we further characterized the interaction among these molecules. As shown

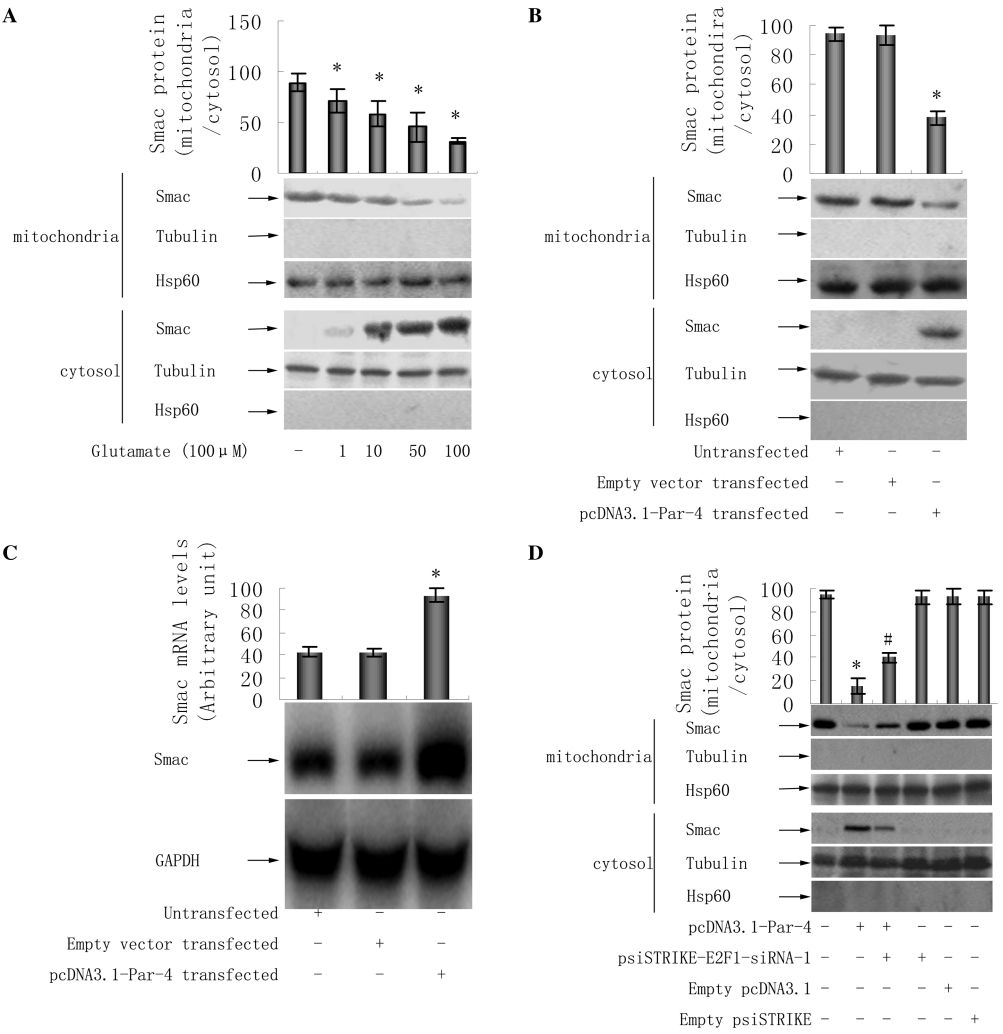

Figure 2. Ectopic expression of Par-4 enhanced Smac protein and transcript. Blocking endogenous E2F1 abrogated the enhancement of Par-4-induced Smac expression. (**A**) Glutamate induced a release of Smac from mitochondria. hBMSCs were treated with glutamate at the dose from 1 to 100 μM. Subcellular localization of Smac was determined by western blotting after 24 h, and protein levels were quantified by computer-assisted densitometry. Tubulin levels were analysed to confirm equal protein loading in cytosol. Hsp60 was used to monitor the absence of mitochondrial contamination in the cytosolic fraction and to verify equal protein loading in mitochondrial fraction. Intensities of bands from western blotting analysis were quantified. Results are indicated as the ratio between Smac levels in mitochondria versus Smac levels in cytosol and are mean ± S.E. of three independent experiments performed in duplicate. $^{*}P < 0.05$ versus the cells without treatment of glutamate. (**B**) Overexpression of Par-4 enhanced Smac protein in hBMSCs. hBMSCs were transfected with either pcDNA3.1-Par-4 or empty pcDNA3.1 vector. Subcellular localization of Smac was determined by Western blotting after 48 h, and protein levels were quantified by computer-assisted densitometry. Tubulin levels were analysed to confirm equal protein loading in cytosol. Hsp60 was used to monitor the absence of mitochondrial contamination in the cytosolic fraction and to verify equal protein loading in mitochondrial fraction. Results are indicated as the ratio between Smac levels in mitochondria versus Smac levels in cytosol and are the mean ± SE of three independent experiments performed in duplicate. $^{*}P < 0.05$ versus the cells transfected with empty vector. (**C**) Overexpression of Par-4 enhanced Smac transcript in hBMSCs. Northern blotting was used to determine Smac mRNA in hBMSCs. hBMSCs were transfected with either pcDNA3.1-Par-4 or empty pcDNA3.1 vector. After 24 h of transfection, total cellular RNAs were separated and hybridized to 32P-labelled DNA probes. GAPDH probe was used to normalize for differences in RNA loading. Intensities of bands from northern blotting analysis were quantitated and normalized with GAPDH. Arbitrary unit = (ASmac/AGAPDH)×100%. Values are mean ± SE of three independent experiments performed in duplicate. $^{*}P < 0.05$ versus the cells transfected with empty vector. (**D**) Blocking endogenous E2F1 by siRNA abrogated the enhancement of Par-4-induced Smac protein in hBMSCs. hBMSCs were co-transfected with pcDNA3.1-Par-4 and psiSTRIKE-E2F1-siRNA-1 vector. As controls, these plasmids or empty vectors were respectively transfected into hBMSCs. Subcellular localization of Smac/DIABLO was determined by western blotting after 48 h, and protein levels were quantified by computer-assisted densitometry. Tubulin protein was analysed to confirm equal protein loading in cytosol. Hsp60 was used to monitor the absence of mitochondrial contamination in the cytosolic fraction and to verify equal protein loading in mitochondrial fraction. Intensities of bands from western blotting analysis were quantitated. Results are indicated as the ratio between Smac levels in mitochondria versus Smac levels in cytosol and are the mean ± S.E. of three independent experiments performed in duplicate. $^{*}P < 0.05$ versus untransfected cells (the first bar at left). $^{*}P < 0.05$ versus hBMSCs transfected only with pcDNA3.1-Par-4. (**E**) Blocking endogenous E2F1 by siRNA abrogated enhancement of Par-4-induced Smac transcript in hBMSCs. hBMSCs were co-transfected with pcDNA3.1-Par-4 and psiSTRIKE-E2F1-siRNA-1 vector. As a control, empty vector was respectively transfected into hBMSCs. After 24 h of transfection, relative amount of Par-4 mRNA was measured by real-time quantitative RT–PCR and normalized against GAPDH. Bars depict the percentage of Par-4 mRNA versus that of untransfected cells. Values are mean ± SE of three independent experiments. $^{*}P < 0.05$ versus untransfected cells (control, the first bar at left). $^{\#}P < 0.05$ versus transfected cells only with pcDNA3.1-*Par-4*.

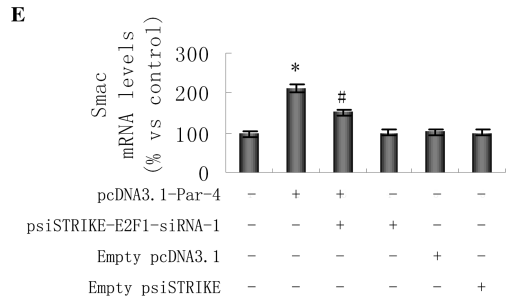

Figure 2. Continued.

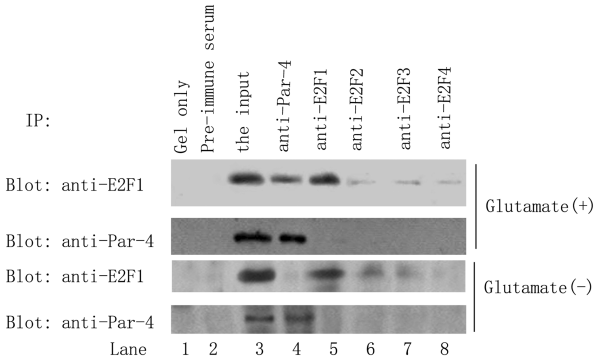

Figure 3. Glutamate induced the formation of protein complex containing *Par-4* and E2F1. Immunoprecipitations and western blotting analysis were performed with whole-cell extracts in hBMSCs with or without treatment of 100 μM glutamate for 24 h. The whole-cell extracts (0.15 mg protein/0.5 ml), were mixed with 10 μl of anti-*Par-4* antibody or preimmune serum. The mixtures were incubated at 4°C for 1 h, and then 10 μl protein A Sepharose beads were added. The mixtures were incubated for 1 h and, after being washed, the beads were submitted for western blotting analysis with anti-E2F1 antibody. Immunoprecipitations with E2F1 antibody and Western blotting with *Par-4* antibody were similarly performed. The other E2F1 family members were used as control.

in Figure 3, *Par-4* co-immunoprecipitated with E2F1 protein in nuclear extracts from the glutamate-treated hBMSCs, indicating the direct interaction between *Par-4* and E2F1. By contrast, in nuclear extracts from the hBMSCs without the treatment of glutamate, *Par-4* failed to associate with E2F1. These data suggested that glutamate induced the formation of protein complex containing *Par-4* and E2F1.

It was E2F1, not *Par-4*, which directly bound to *Smac* promoter in Par-4-E2F1 complex, and *Par-4* exerted its transcriptional control on *Smac* gene through indirect interacting with E2F1

Next, we used a previously identified E2F1-binding site BS3 (−200 to −193 bp relative to ATG) on the *Smac* promoter as bait to pull out potential interacting molecules (12). This *Smac* promoter sequence was labelled with biotin using terminal deoxynucleotidyltransferase and incubated with nuclear extracts from hBMSCs treated with or without 100 μM glutamate for 24 h. Following this, the samples were subjected to high salt washes to remove any non-specific binding. The washed complex was pulled out, using streptavidin conjugated to magnetic beads, with the help of a magnet. The proteins binding to the promoter were eluted by boiling in Laemmli's buffer and subjected to SDS–PAGE, and Western blotting for *Par-4* was performed using anti-*Par-4* antibody. Indeed, we found that *Par-4* and E2F1 existed in nuclear extracts from glutamate-treated cells (Figure 4A, lane 1; Figure 4B, lane 1). The *Par-4*-specific antibody (R334) has been shown previously (28) to disrupt the interaction between *Par-4* and other molecules. We could not almost detect *Par-4* in the nuclear extracts preincubated with the R334 antibody and then incubated with the biotin-labeled E2F1-binding site on *Smac* promoter (Figure 4A, lane 2). Similarly, E2F1 also decreased markedly upon the pre-incubation of the neutralizing antibody against E2F1 (Figure 4B, lane 2). Together, this set of experiments indicated that *Par-4* and E2F1 bound either indirectly or directly to *Smac* promoter in glutamate-treated hBMSCs.

To further elucidate the molecular mechanisms by which *Par-4* and E2F1 interact with the *Smac* promoter, EMSA experiments *in vitro* were performed with the nuclear extracts from hBMSCs treated with glutamate. Previously defined E2F1-binding site BS3 (−200 to −193 bp relative to ATG) on *Smac* promoter were used as probes (12). Two complexes were formed with the BS3 oligonucleotide (Figure 4C, lane 2). Competition with increasing amounts of cold competitor demonstrated that both complexes were specific (Figure 4C, lane 3). To determine the presence of *Par-4* and E2F1 in the complexes formed, nuclear extracts from the glutamate-treated hBMSCs were incubated with the BS3 probe along with antibodies directed against *Par-4* or E2F1. The anti-*Par-4* antibody is directed against the COOH terminus of *Par-4* and has been demonstrated previously as a blocking antibody (28). The anti-*Par-4* antibody caused disappearance of the slower migrating complex, indicating the presence of *Par-4* (Figure 4C, lane 4). The neutralizing antibody against E2F1 caused disappearance of both the faster and the slower migrating complex, thus indicating the presence of E2F1 in both the complexes (Figure 4C, lane 5). These results supported that it was E2F1, not *Par-4*, in *Par-4*-E2F1 proteins complex that directly bound to *Smac* promoter, and that *Par-4* might indirectly exert its transcriptional control on *Smac* gene though interacting with E2F1. The BS3 E2F1-binding site was also used as a probe to perform EMSA with nuclear extracts from the hBMSCs without treatment of glutamate. However, no DNA–protein complex was found (Figure 4C, lane 7). Therefore, the presence of glutamate was critical for the formation of these DNA–protein complexes.

Par-4-E2F1 complex bound to the BS3 Site (−200 to−193 bp relative to ATG) within *Smac* promoter in glutamate-treated hBMSCs *in vivo*

To evaluate directly the potential significance of physical interactions among *Par-4*, E2F1 and *Smac* promoter, we investigated whether *Par-4* and E2F1 associate on the chromatin of endogenous *Smac* promoter using the chromatin immunoprecipitation assay. We immunoprecipitated chromatin from the glutamate-treated hBMSCs, using specific antibodies against *Par-4* and E2F1 or no

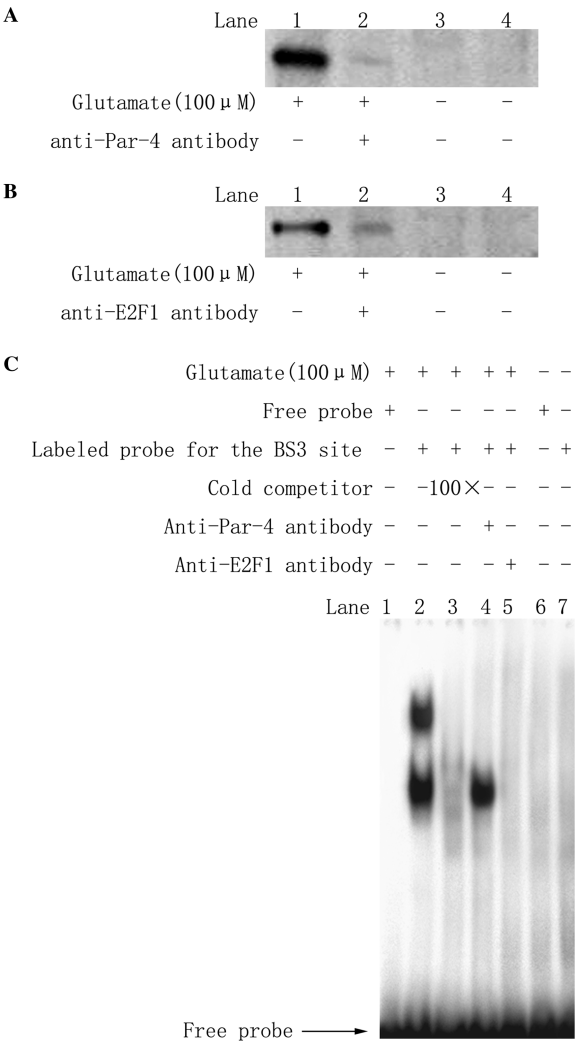

Figure 4. *Par-4* and E2F1 bound to *Smac* promoter in hBMSCs with exposure of glutamate. (**A** and **B**) hBMSCs were treated with or without 100 μM glutamate for 24 h. And nuclear proteins were isolated. Before the binding reaction, 50 μg of nuclear extract was preincubated with either anti-*Par-4* antibody (R334) or anti-E2F1 antibody. Subsequently, these nuclear extracts were co-incubated with the magnetic beads containing biotinylated oligonucleotide sequence of SB3 sites within *Smac* promoter for binding reaction. The beads were captured by a magnet, washed three times with a high salt buffer, and resuspended in Laemmli buffer. The samples were heated at 95°C for 5 min to elute all the proteins, loaded onto a 12% SDS–PAGE, electrophoresed, and transferred to a nitrocellulose membrane. *Par-4* and E2F1 were detected using the *Par-4* antibody (R334) or E2F1 antibody by immunoblotting. (**C**) DNA-binding activity of E2F1-binding sites BS3 (−200 to −193 bp) within *Smac* promoter was assessed by electrophoretic mobility shift assay. After treatment with or without 100 μM glutamate for 24 h, nuclear extracts were obtained from the hBMSCs. Nuclear extracts were incubated with the probes in the presence or absence of antibodies directed against *Par-4* or E2F1. In competition studies, a 100-fold molar excess of unlabelled oligonucleotide was added to binding reaction mixture before the addition of the labelled probes. Results shown are representative of three independent experiments.

antibody at all as a control. Genomic DNA fragments bound to *Par-4* or E2F1 were analysed by PCR using primers upstream of the BS3 (−200 to −193 bp relative to ATG) site within *Smac* promoter. Analysis of genomic

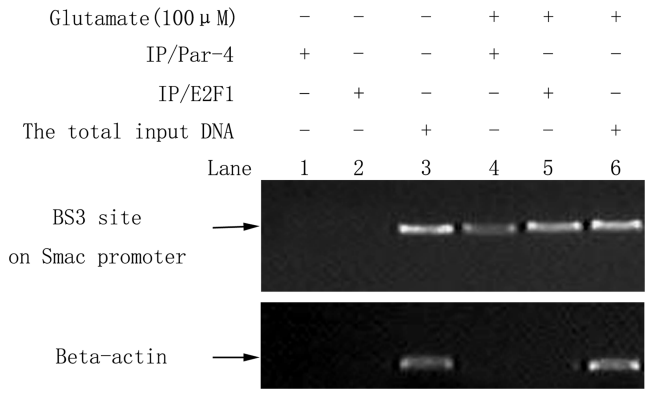

Figure 5. Demonstration of *in vivo* binding of *Par-4* and E2F1 to BS3 site (−200 to −193 bp relative to ATG) on the *Smac/DIABLO* promoter by chromatin immunoprecipitation. hBMSCs were treated with or without 100 μM glutamate for 24 h. Chromatin lysates were immunoprecipitated (IP) with either antibody against *Par-4* or antibody against E2F1. The samples were processed as described under 'Materials and Methods' section. Immunoprecipitated DNA was amplified using primers representing the BS3 site (−200 to−193 bp relative to ATG) on *Smac* promoter. PCR analysis of the total input DNA was also preformed. Products of chromatin immunoprecipitation and PCR amplification were analysed by 2% agarose gel electrophoresis and beta-actin was performed as a negative control. Results are representative of three independent experiments.

DNA immunoprecipitated with anti-*Par-4* antibody revealed *Smac* promoter in glutamate-treated hBMSCs (Figure 5, lane 4). Also, immunoprecipitates from anti-E2F1 antibody revealed the presence of *Smac* promoter (Figure 5, lane 5). As expected, when minus the antibodies in the immunoprecipitation procedure, no genomic DNA was pulled out (Figure 5, lane 6). Chromatin immunoprecipitated with anti-*Par-4* antibody or anti-E2F1 antibody was subjected to PCR using primers representing BS2 (−542 to −535 bp relative to ATG) site, another previously reported E2F1-binding site. No DNA could be amplified from the chromatins, (data not shown), demonstrating that *Par-4* and E2F1 specifically bind to the BS3 (−200 to −193 bp relative to ATG) site on the *Smac* promoter. In addition, we did not observe any *Smac* promoter pulled down by anti-*Par-4* or anti-E2F1 antibody in hBMSCs without exposure to glutamate. Together, these findings strongly support the idea that *Par-4* and E2F1 interact with a previously defined BS3 site within *Smac* promoter *in vivo* in glutamate-treated hBMSCs.

The indirect transcriptional regulation of *Par-4* on *Smac* was dependant on its COOH terminus-mediated interaction between *Par-4* and E2F1 in hBMSCs

To identify structural determinants of *Par-4* responsible for its regulatory function on *Smac* transcription, we focused on investigating the role of the COOH terminus of *Par-4*, since a stretch of 70 amino acids at this region showed homology to a domain referred to as the death domain, which was also found in other pro-apoptotic proteins such as Fas, FADD and TNFR-1 (6,20). We engineered and constructed plasmids pcDNA3.1-myc-*Par-4* and pcDN3.1-myc-Δ*Par-4*, encoding a myc fusion protein

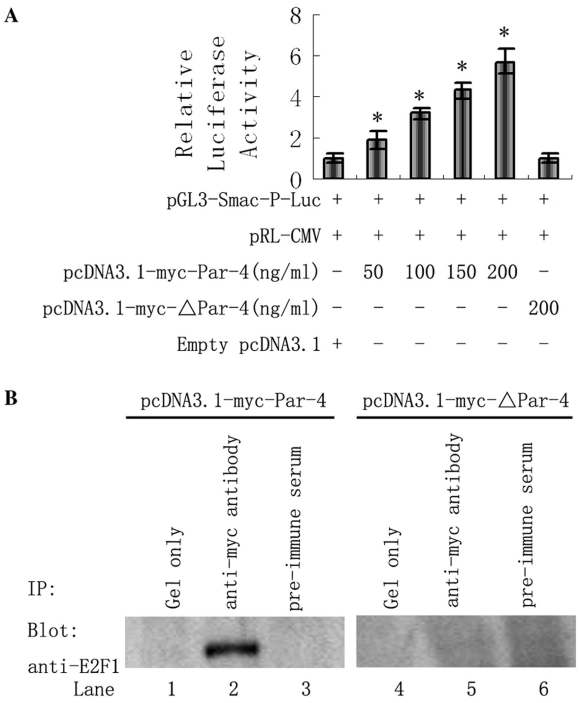

Figure 6. The indirectly regulation of *Par-4* on *Smac*/*DIABLO* promoter was dependant on its COOH terminus-mediated interaction between *Par-4* and E2F1 in the hBMSCs. (**A**) Luciferase activity assays. hBMSCs were co-transfected with pGL3-Smac-P-Luc reporter and pRL-CMV vector as an internal control for transfection efficiency. At the same time the cells were also transfected with either increasing amounts of pcDNA3.1-myc-*Par-4* or pcDNA3.1-myc-Δ*Par-4*, or an empty pcDNA3.1 vector. Luciferase activity was determined at 24 h after transfection. Non-transfected cells were used as the background. All values were normalized for expression of *Renilla* luciferase and expressed as X-fold induction relative to the activity of pGL3-*Smac*-P-Luc reporter co-transfected with empty pcDNA3.1. Shown is a representative experiment of three independent experiments. Values are mean ± SE of three independent experiments. $^{*}P < 0.05$ versus cells co-transfected with pGL3-*Smac*-P-Luc reporter and empty pcDNA3.1. (**B**) Immunoprecipitations and Western blotting analysis of nuclear extracts in hBMSCs. Cells was transfected with pcDNA3.1-myc-*Par-4* or pcDNA3.1-myc-Δ*Par-4*. After 24 h of transfection, nuclear proteins were extracted. Then the nuclear extracts, (0.15 mg protein/0.5 ml), were mixed with 10 μl of anti-myc antibody or pre-immune serum. The mixtures were incubated at 4°C for 1 h, and then 10 μl protein A Sepharose beads were added. The mixtures were incubated for 1 h and, after being washed, the beads were submitted for western blotting analysis with anti-E2F1 antibody. Lanes 1 and 4, protein A gel only; lanes 2 and 5, cell lysate immunoprecipitated with anti-myc antibody; lanes 3 and 6, cell lysate incubated with pre-immune serum.

containing full-length *Par-4* protein or a deletion mutant, respectively, of which the latter lacked 70 amino acids at the COOH terminus. Then, pGL3-*Smac*-P-Luc reporter, which contained *Smac* promoter fragment (−600 to −100 bp relative to ATG), was cotransfected into hBMSCs with pcDNA3.1-myc-*Par-4* or pcDNA3.1-myc-Δ*Par-4*. Equal concentrations of *Renilla* reporter plasmid pRL-CMV were also co-introduced into cells as an internal control. Luciferase activities were measured and pGL3-*Smac*-P-Luc reporter activities normalized to pRL-CMV internal standard were presented in the histogram with arbitrary units. As shown in Figure 6A, cotransfection with increasing amounts of full-length *Par-4* resulted in an increased activity of *Smac* promoter in a dose-dependent manner, whereas mutant *Par-4* or empty vector failed to give rise to noticeable activation of *Smac* promoter. These data indicated the COOH terminus of *Par-4* was essential for *Par-4*-mediated activation of *Smac* promoter.

Although, as delineated previously (15), no evidence was provided that *Par-4* could directly bind to DNA molecule, our above studies has demonstrated that *Par-4* and E2F1 could form protein complex and bind to *Smac* promoter. Hence, we could set up a hypothesis that the COOH terminus of *Par-4* might contribute to proteins complex formation of *Par-4* and E2F1, and then via recruitment of E2F1 to *Smac* promoter, *Par-4* induced indirectly *Smac* transcription. In order to further corroborate this hypothesis, we performed the co-immunoprecipitation assays for measuring the interaction between *Par-4* and E2F1. As shown in Figure 6B (lane 2), from nuclear extracts of the cells transfected with pcDNA3.1-myc-*Par-4* and following treated with glutamate, myc-*Par-4* was immunoprecipitated using anti-myc antibody, and associated E2F1 were detected by immunoblotting. However, *Par-4* deletion mutant, which lacked the COOH terminus of wild-type *Par-4* protein, failed to associate with E2F1 (Figure 6B, lane 5). The findings validated the essentiality of the COOH terminus of *Par-4* for *Par-4*-E2F1 complex formation. Taken together, we concluded that the COOH terminus of *Par-4*, by which *Par-4* associated with E2F1 and bound to *Smac* promoter, was functionally required for *Par-4*-mediated activation of *Smac* promoter in hBMSCs.

DISCUSSION

In this study, we report for the first time that glutamate can induce apoptosis in hBMSCs by a mechanism involving pro-apoptotic gene *Par-4*. Glutamate-induced neurotoxicity is an important contributor in acute neuronal damages and in chronic neurodegenerative diseases (16,17). Therefore, implanted stem cells will be sure to suffer from glutamate-mediated injury. We observed that glutamate induced a dose- and time-dependent apoptosis in hBMSCs, which was consistent with previous studies carried out in neural cells (4,16–18). As a pro-apoptotic factor, *Par-4* is initially identified as a product of gene upregulated in prostate tumour cells undergoing apoptosis (5). Recently, growing evidence show that increased expression of *Par-4* also regulates neuronal apoptosis, especially when exposed to metabolic insults such as glutamate and intracellular calcium elevation (15,19). In the current study, we demonstrated that the suppression of *Par-4* expression greatly attenuated apoptosis in glutamate-treated hBMSCs, whereas *Par-4* overexpression increased the percentage of apoptotic cells, implying that *Par-4* played a critical role in glutamate-induced hBMSCs apoptosis.

Previously, several signal pathways, including WT1/Bcl-2, Fas/Fas ligand, PKC/p38 mitogen-activated protein kinase (MAPK), Ras/NF-kB, DAP-like or ZIP kinase

(DIK/ZIP kinase), extracellular signal regulated-kinase (ERK), have been demonstrated to be involved in *Par-4*-mediated apoptosis (6,9,20,21). Our studies showed that *Par-4* ectopic expression in hBMSCs resulted in increased release of *Smac* protein from mitochondria and elevation of *Smac* message RNA, suggesting a previously undefined transcriptional mechanism for *Par-4*-mediated *Smac* upmodulation. However, previous studies did not provide any evidence to support the direct interaction between *Par-4* protein and *Smac* promoter. Our data showed that blocking endogenous E2F1 decreased *Par-4*-induced *Smac* transcription, indicating that both *Par-4* and E2F1 were required for *Smac* transcription regulation. Numerous studies showed that ectopic expression of E2F1 induced apoptosis by different mechanisms. Apoptosis-related E2F1 target genes, such as *p73*, *Apaf1*, *noxa*, *bim* and *akt*, are involved in both p53-dependent and p53-independent apoptotic regulation (22–27). A recent study demonstrated that enhanced accumulation of nuclear E2F1 upregulated *Smac* expression and subsequently accelerated mitochondria-mediated apoptosis, implying that *Smac* was an E2F1 target gene (12). In agreement with the study, our data showed that the increased expression of *Smac* gene in glutamate-treated hBMSCs were E2F1-dependent, at least partially.

We further confirmed that both *Par-4* and E2F1 proteins participated in the formation of a complex that bound to the BS3 site (−200 to −193 bp relative to ATG) on *Smac* promoter, which was previously identified as a site where E2F1 bound to and increased transcription of *Smac* gene in human H1299 non-small lung carcinoma cells (12). Our results indicated that this site was also employed to drive the transcription of *Smac* in hBMSCs. Similar mechanism of *Par-4* mediated indirect transcriptional regulation was delineated by Sangeeta and colleagues as well. They demonstrated that *Par-4* associated with WT1 and bound to the bcl-2 promoter to transcriptionally regulate Bcl-2 expression in an androgen-independent prostate cancer cell line (28). In particular, our results suggested that it was E2F1, not *Par-4*, that directly bound to *Smac* promoter in the DNA–proteins complex, which implied that *Par-4*, indirectly, exert its transcriptional control on *Smac* gene though interacting with E2F1.

Consistent with previous studies (6,20), our study validated the functional significance of the COOH terminus of *Par-4* protein in hBMSCs apoptosis. The COOH terminus of *Par-4* protein containing a leucine zipper domain has been shown to be essential in *Par-4* binding to PKC, WT1, ZIPK/Daxx and THAP, and their interactions promoted cell apoptosis (6,20,29). Here we showed that the mutant of *Par-4*, which lacked 70 amino acids at the COOH terminus, failed to co-immunoprecipitate with E2F1 protein, implying that this region was also required for the interaction between *Par-4* and E2F1. With luciferase activity analysis, we found that the increased expression of *Par-4* resulted in an increased activity of *Smac* promoter in a dose-dependent manner, whereas *Par-4* mutant failed to active *Smac* promoter. Therefore, we further corroborated that the indirect transcripional regulation of *Par-4* on *Smac* was depended on its COOH terminus-mediated interaction between *Par-4* and E2F1.

Recently, it was reported that the COOH terminus of or possibly the full-length *Par-4* protein was not required for apoptosis in primary fibroblasts (30). This discrepancy may be due to the different cell types, since in the same experiment settings, depletion of *Par-4* in HeLa cells conferred a significant resistant to various apoptotic agents (30).

In summary, we show that the proteins–DNA complex, containing *Par-4* protein, E2F1 protein and *Smac* promoter, contributes to glutamate-induced apoptosis in hBMSCs. The *Par-4* mediated indirect transcripional regulation on *Smac* gene depended on its COOH terminus-mediated interaction between *Par-4* and E2F1. Our studies provide a further understanding of molecular mechanism in glutamate induced hBMSCs apoptosis, which benefit stem-cell therapy in ischemic brain damage.

SUPPLEMENTARY DATA

Supplementary Data are available at NAR Online.

ACKNOWLEDGEMENTS

This work was supported by Medical Grants of Scientific and Technological Development from the Health Department of Jiangsu Province in China (No. K200504), National Natural Science Foundation of China (30570863) and the Medical Academic Key Talent Program of Jiangsu Province in China (RC2007050). Funding to pay the Open Access publication charges for this article was provided by the first Affiliated Hospital of Nanjing Medical University.

Conflict of interest statement. None declared.

REFERENCES

1. Goldstein,L.B. (2007) Acute ischemic stroke treatment in 2007. *Circulation*, **116**, 1504–1514.
2. Svan der Worp,H.B. and van Gijn,J. (2007) Acute ischemic stroke. *N Engl J Med*, **357**, 572–579.
3. Folkerth,R.D. (2007) The neuropathology of acquired pre- and perinatal brain injuries. *Semin. Diagn. Pathol.*, **24**, 48–57.
4. Bano,D. and Nicotera,P. (2007) Ca2+ signals and neuronal death in brain ischemia. *Stroke*, **38**, 674–676.
5. Qiu,G., Ahmed,M., Sells,S.F., Mohiuddin,M., Weinstein,M.H. and Rangnekar,V.M. (1999) Mutually exclusive expression patterns of Bcl-2 and Par-4 in human prostate tumors consistent with down-regulation of Bcl-2 by Par-4. *Oncogene*, **18**, 623–631.
6. Johnstone,R.W., See,R.H., Sells,S.F., Wang,J., Muthukkumar,S., Englert,C., Haber,D.A., Licht,J.D., Sugrue,S.P., Roberts,T. *et al.* (1996) A novel repressor, par-4, modulates transcription and growth suppression functions of the Wilms' tumor suppressor WT1. *Mol. Cell Biol.*, **16**, 6945–6956.
7. Diaz-Meco,M.T., Municio,M.M., Frutos,S., Sanchez,P., Lozano,J., Sanz,L. and Moscat,J. (1996) The product of par-4, a gene induced during apoptosis, interacts selectively with the atypical isoforms of protein kinase C. *Cell*, **86**, 777–786.
8. Kogel,D.O., Plottner,O., Landsberg,G., Christian,S. and Scheidtmann,K.H. (1998) Cloning and characterization of Dlk, a novel serine/threonine kinase that is tightly associated with chromatin and phosphorylates core histones. *Oncogene*, **17**, 2645–2654.

9. Dutta,K., Alexandrov,A., Huang,H. and Pascal,S.M. (2001) pH-induced folding of an apoptotic coiled coil. *Protein Sci.*, **10**, 2531–2540.
10. Shiozaki,E.N. and Shi,Y. (2004) Caspases, IAPs and Smac/DIABLO: mechanisms from structural biology. *Trends Biochem. Sci.*, **29**, 486–494.
11. Degli Esposti,M. (2004) Mitochondria in apoptosis: past, present and future. *Biochem. Soc. Trans.*, **32**, 493–495.
12. Xie,W., Jiang,P., Miao,L., Zhao,Y., Zhimin,Z., Qing,L., Zhu,W.G. and Wu,M. (2006) Novel link between E2F1 and Smac/DIABLO: proapoptotic Smac/DIABLO is transcriptionally upregulated by E2F1. *Nucleic Acids Res.*, **34**, 2046–2055.
13. Moriscot,C., de Fraipont,F., Richard,M.J., Marchand,M., Savatier,P., Bosco,D., Favrot,M. and Benhamou,P.Y. (2005) Human bone marrow mesenchymal stem cells can express insulin and key transcription factors of the endocrine pancreas developmental pathway upon genetic and/or microenvironmental manipulation in vitro. *Stem Cells*, **23**, 594–603.
14. Byung-Chul,K., Howard van,G., Tae,A.K., Ho-Jae,L, Kim,G.B., Hyun,H.C., David,A.L., Kyeong,S.C. and Seong-Jin,K. (2004) Activin Receptor-like Kinase-7 Induces Apoptosis through Activation of MAPKs in a Smad3-dependent Mechanism in Hepatoma Cells. *J. Biol. Chem.*, **279**, 28458–28465.
15. El-Guendy,N. and Rangnekar,V.M. (2003) Apoptosis by Par-4 in cancer and neurodegenerative diseases. *Exp. Cell Res.*, **283**, 51–66.
16. Hazell,A.S. (2007) Excitotoxic mechanisms in stroke: an update of concepts and treatment strategies. *Neurochem. Int.*, **50**, 941–953.
17. Pirondi,S., Fernandez,M., Schmidt,R., Hokfelt,T., Giardino,L. and Calza,L. (2005) The galanin-R2 agonist AR-M1896 reduces glutamate toxicity in primary neural hippocampal cells. *J. Neurochem.*, **95**, 821–833.
18. Ohno-Shosaku,T., Hashimotodani,Y., Ano,M., Takeda,S., Tsubokawa,H. and Kano,M. (2007) Endocannabinoid signalling triggered by NMDA receptor-mediated calcium entry into rat hippocampal neurons. *J. Physiol.*, **584**, 407–418.
19. Duan,W., Rangnekar,V.M. and Mattson,M.P. (1999) Prostate apoptosis response-4 production in synaptic compartments following apoptotic and excitotoxic insults: evidence for a pivotal role in mitochondrial dysfunction and neuronal degeneration. *J. Neurochem.*, **72**, 2312–2322.
20. Xie,J. and Guo,Q. (2005) PAR-4 is involved in regulation of beta-secretase cleavage of the Alzheimer amyloid precursor protein. *J. Biol. Chem.*, **280**, 13824–13832.
21. Goswami,A., Ranganathan,P. and Rangnekar,V.M. (2006) The phosphoinositide 3-kinase/Akt1/Par-4 axis: a cancer-selective therapeutic target. *Cancer Res.*, **66**, 2889–2892.
22. Eymin,B., Karayan,L., Seite,P., Brambilla,C., Brambilla,E., Larsen,C.J. and Gazzeri,S. (2001) Human ARF binds E2F1 and inhibits its transcriptional activity. *Oncogene*, **20**, 1033–1041.
23. Datta,A., Nag,A. and Raychaudhuri,P. (2002) Differential regulation of E2F1, DP1, and the E2F1/DP1 complex by ARF. *Mol. Cell Biol.*, **22**, 8398–8408.
24. Stiewe,T. and Putzer,B.M. (2000) Role of the p53-homologue p73 in E2F1-induced apoptosis. *Nature Genet.*, **26**, 464–469.
25. Moroni,M.C., Hickman,E.S., Lazzerini,D. E., Caprara,G., Colli,E., Cecconi,F., Muller,H. and Helin,K. (2001) Apaf-1 is a transcriptional target for E2F and p53. *Nature Cell Biol.*, **3**, 552–558.
26. Furukawa,Y., Nishimura,N., Furukawa,Y., Satoh,M., Endo,H., Iwase,S., Yamada,H., Matsuda,M., Kano,Y. and Nakamura,M. (2002) Apaf-1 is a mediator of E2F-1-induced apoptosis. *J. Biol. Chem.*, **277**, 39760–39768.
27. Chaussepied,M. and Ginsberg,D. (2004) Transcriptional regulation of AKT activation by E2F. Mol. *Cell*, **16**, 831–837.
28. Cheema,S.K., Mishra,S.K., Rangnekar,V.M., Tari,A.M., Kumar,R. and Lopez-Berestein,G. (2003) Par-4 Transcriptionally Regulates Bcl-2 through a WT1-binding Site on the bcl-2 Promoter. *J. Biol. Chem.*, **278**, 19995–20005.
29. Wang,G., Silva,J., Krishnamurthy,K., Tran,E., Condie,B.G. and Bieberich,E. (2005) Direct binding to ceramide activates protein kinase Czeta before the formation of a pro-apoptotic complex with PAR-4 in differentiating stem cells. *J. Biol. Chem.*, **280**, 26415–26424.
30. Affar el,B., Luke,M.P., Gay,F., Calvo,D., Sui,G., Weiss,R.S., Li,E. and Shi,Y. (2006) Targeted ablation of Par-4 reveals a cell type-specific susceptibility to apoptosis-inducing agents. *Cancer Res.*, **66**, 3456–3462.